Mechanism of Oxime Reactivation of Acetylcholinesterase Analyzed by Chirality and Mutagenesis†

Lilly Wong,‡ Zoran Radić,‡ Roger J. M. Brüggemann,‡,§ Natilie Hosea,‡,|| Harvey A. Berman,⊥ and Palmer Taylor*,‡

Department of Pharmacology, University of California, San Diego, La Jolla, California 92093-0636, and Department of Biochemical Pharmacology, State University of New York at Buffalo, Buffalo, New York 14260

Received December 20, 1999; Revised Manuscript Received March 8, 2000

ABSTRACT: Organophosphates inactivate acetylcholinesterase by reacting covalently with the active center serine. We have examined the reactivation of a series of resolved enantiomeric methylphosphonate conjugates of acetylcholinesterase by two oximes, 2-pralidoxime (2-PAM) and 1-(2′-hydroxyiminomethyl-1′-pyridinium)-3-(4′-carbamoyl-1-pyridinium) (HI-6). The S_p enantiomers of the methylphosphonate esters are far more reactive in forming the conjugate with the enzyme, and we find that rates of oxime reactivation also show an S_p versus R_p preference, suggesting that a similar orientation of the phosphonyl oxygen toward the oxyanion hole is required for both efficient inactivation and reactivation. A comparison of reactivation rates of (S_p)- and (R_p)-cycloheptyl, 3,3-dimethylbutyl, and isopropyl methylphosphonyl conjugates shows that steric hindrance by the alkoxy group precludes facile access of the oxime to the tetrahedral phosphorus. To facilitate access, we substituted smaller side chains in the acyl pocket of the active center and find that the Phe295Leu substitution enhances the HI-6-elicited reactivation rates of the S_p conjugates up to 14-fold, whereas the Phe297Ile substitution preferentially enhances 2-PAM reactivation by as much as 125-fold. The fractional enhancement of reactivation achieved by these mutations of the acyl pocket is greatest for the conjugated phosphonates of the largest steric bulk. By contrast, little enhancement of the reactivation rate is seen with these mutants for the R_p conjugates, where limitations on oxime access to the phosphonate and suboptimal positioning of the phosphonyl oxygen in the oxyanion hole may both slow reactivation. These findings suggest that impaction of the conjugated organophosphate within the constraints of the active center gorge is a major factor in influencing oxime access and reactivation rates. Moreover, the individual oximes differ in attacking orientation, leading to the presumed pentavalent transition state. Hence, their efficacies as reactivating agents depend on the steric bulk of the intervening groups surrounding the tetrahedral phosphorus.

Reaction of organophosphates with the serine hydrolase family of enzymes such as acetylcholinesterase (AChE)[1] is characterized by the formation of the serine-conjugated phosphonates or phosphorates which are only slowly reversible. The classic studies of Irwin Wilson and his colleagues some 40 years ago demonstrated that strong nucleophiles such as oximes are able to reactivate organophosphate−cholinesterase conjugates, giving rise to free enzyme (*1*−*3*). The strength of the nucleophile, the orientation of the nucleophile with respect to the phosphate conjugated to the active center serine, and prevention of aging of the organophosphate conjugate are three factors well known to affect reactivation. Relying on the first two considerations, various oximes were subsequently developed as antidotes to cholinesterase poisoning (*2*, *3*). One of the limitations to the use of oximes is the relatively slow rate of reactivation they elicit, and an understanding of the mechanism of reactivation might lead to means by which reactivation rates can be enhanced. By contrast, aging arises from cleavage of the carbon−oxygen bond on one of the alkoxy constituents on the conjugated organophosphate, resulting in an anionic phosphylated conjugate resistant to all oximes.

Early studies demonstrated chiral preferences at the phosphorus moiety and at the attached alkyl carbons for rates of inactivation by the organophosphates (*4*−*8*). Moreover, oxime reactivation kinetics also appear to show structural (*9*) and chiral preferences for the attached organophosphate (*10*, *11*). While these studies point to orientational constraints for organophosphate attack of the active center serine and oxime attack of the phosphoserine, details on ligand accessibility to the active center awaited a structure of the enzyme.

The availability of three-dimensional structures of AChE (*12*−*14*) provided an expanded framework for examining the mechanism of the organophosphate inactivation (*15*−*18*) and oxime reactivation (*19*, *20*). The active center and site of conjugation by organophosphates lie at the base of a narrow gorge some 18−20 Å in depth. The largely aromatic side chains lining the gorge wall and contributing to the acyl

† Supported by Grants USPHS GM18360 to P.T. and DAMD 17C 95I-5027 and USPHS ES-03085 to H.A.B.

‡ University of California.

§ Present address: Department of Medicinal Chemistry, University of Utrecht, The Netherlands.

|| Present address: Central Research, Pfizer, Groton, CT 06340.

⊥ State University of New York at Buffalo.

[1] Abbreviations: AChE, acetylcholinesterase; 2-PAM, pralidoxime iodide; obidoxime, 1,1′-(oxymethylene)bis[4-(hydroxyimino)methylpyridinium]; DDVP, *O*,*O*-dimethyl *O*-(2,2-dichlorovinyl)phosphate; HI-6, 1-(2′-hydroxyiminomethyl-1′-pyridinium)-3-(4′-carbamoyl-1-pyridinium).

10.1021/bi992906r CCC: $19.00 © 2000 American Chemical Society
Published on Web 04/21/2000

pocket and the choline binding subsite at the base of the gorge are well defined. Thus, diffusional entry of the ligand within the narrow confines of the gorge and the orientation of the associated and conjugated ligands become important considerations.

Recently, using a series of resolved (S_p)- and (R_p)-alkylmethylphosphonyl thiocholines and neutral thioates, we examined the influence of acyl pocket dimensions and charges of residues in the gorge on the rates of phosphonylation. From this approach, we ascertained the determinants responsible for the chiral preference of (S_p)- and (R_p)-phosphonates (*15*−*17*) and for the reaction specificity of organophosphates with cationic and neutral leaving groups (*16*). With the structure of the active center of the AChE templates known and the absolute stereochemistry of the phosphonates assigned, the configuration of the reactant phosphonate in the transition state can be predicted (*17*).

In this study, we combine measurements of the chiral preference of the organophosphate for reactivation by oximes with modification of the acyl pocket dimensions by site-specific mutagenesis to examine the orientation of the attacking oxime in the reaction. Using a series of congeneric (R_p)- and (S_p)-methylphosphonates conjugated to the active center, we show that impaction of the organophosphate in the narrow gorge restricts access of the oxime to the phosphonate and individual oximes attack from distinct angles. For the S_p enantiomers, steric constraints within the gorge can be relieved, in part, by substitution of smaller alkyl residues for the large aromatic residues in the acyl pocket, such that reactivation rates are markedly enhanced. Steric constraints may prevent the R_p enantiomers from maintaining a low-energy conformation with their phosphonyl oxygen in the oxyanion hole; association with the oxyanion hole may facilitate both efficient inactivation and reactivation.

MATERIALS AND METHODS

Materials. Synthesis, characterization, and determination of the absolute stereochemistry of the (R_p)- and (S_p)-alkylmethylphosphonyl thiocholines have been described previously (*6*, *7*). 2-PAM (2-pralidoxime iodide) was a product of Sigma; HI-6 [1-(2′-hydroxyiminomethyl-1′-pyridinium)-3-(4′-carbamoyl-1-pyridinium)] and obidoxime [1,1′-(oxymethylene)bis[4-(hydroxyimino)methylpyridinium] were gifts from B. P. Doctor at Walter Reed Medical Center (Washington, DC). DDVP [*O*,*O*-dimethyl *O*-(2,2-dichlorovinyl)phosphate] was a generous gift of R. Fanelli (Bayer, Inc., West Haven, CT). Structures of the alkyl phosphates and oximes used in this study are shown in Figure 1. AChE was produced by transfection of an expression plasmid encoding the 548 amino-terminal amino acids in mouse AChE into human embryonic kidney (HEK-293) cells, selection of expressing cells, and expression as a secreted, soluble enzyme in the culture media (*15*). Purification and characterization of wild-type and F295L and F297I mutant AChEs are described in detail in previous studies (*22*).

Reaction Kinetics. Wild-type and mutant enzymes were reacted with a slight stoichiometric excess of the corresponding alkylphosphonate until the extent of inhibition of ACh hydrolysis was greater than 95%. Inhibited AChE ($\sim 10^{-5}$−10^{-6} M) was passed through a Sephadex G-50 spin column (Pharmacia) to remove excess unconjugated reactants, incubated with oxime in 10 mM Tris-HCl buffer (pH 8) containing 40 mM $MgCl_2$ and 100 mM NaCl, and diluted 1:1000, and residual activity was measured by the Ellman assay (*23*).

Nucleophilic reactivation of organophosphate-inhibited AChE is thought to proceed through the following mechanism (*1*, *2*, *24*, *25*).

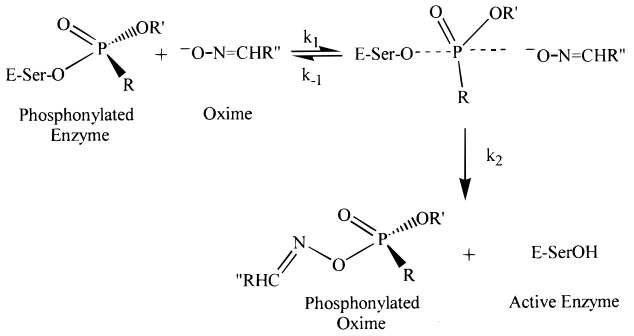

The reaction rate constant, k_{obs}, describing regeneration of E−SerOH can be described in terms of an apparent equilibrium constant, K_{ox}, and an intrinsic reaction constant, k_2.

$$k_{obs} = \frac{k_2}{1 + K_{ox}/[\text{oxime}]} \quad (1)$$

where

$$k_r = k_2/K_{ox} \quad (2)$$

and

$$K_{ox} = \frac{k_{-1} + k_2}{k_1} \quad (3)$$

When $k_2 < k_{-1}$, $K_{ox} = k_{-1}/k_1$ and thus reflects the dissociation constant of the oxime from the phosphonylated enzyme. The phosphonyl oxime product is also known to be inhibitory to the enzyme (*25*), but it should not accumulate, by virtue of the initial removal of excess organophosphate. Hence, phosphonyl oxime concentrations should not exceed the enzyme (1 nM), concentrations shown not to be inhibitory for the phosphonyl conjugates of HI-6 and 2-PAM (*25*).

Data were plotted in terms of fractional reactivation as a function of time. Full reactivation was achieved by passing an equivalent sample of uninhibited AChE through a parallel column to account for dilution.

Structures of the Conjugated Alkyl Methylphosphonates and the Oximes. Structures of the (R_p)- and (S_p)-alkyl methylphosphonates and the achiral dimethyl phosphorate conjugated to AChE were built using the Insight II and MOPAC optimization programs. Oxime structures were obtained from the Cambridge Structural Data Base (*26*).

Starting configurations of the conjugated phosphonates were built from congeneric organophosphates whose structures were found in the Cambridge Data Base. The AChE−organophosphate conjugate was formed by deletion of the leaving group and placement of the serine γ-oxygen a covalent bond distance ($\leq$3 Å) from the phosphate. The structures were then minimized by steepest descent prior to an estimation of the charge distribution. The ab initio

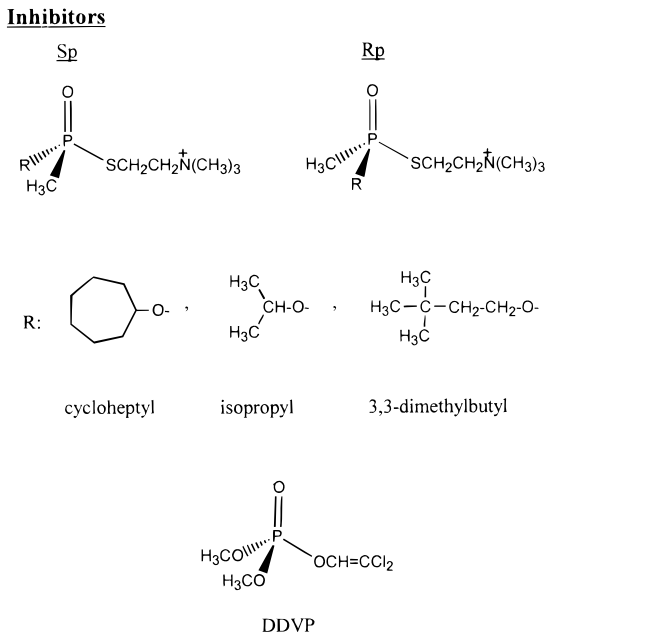

FIGURE 1: Structures of the organophosphates and oximes used in this study. Upon reaction of the organophosphates with the active site serine, thiocholine and dichloroethylene are the two leaving groups forming the respective phosphoserine (203) conjugates of the enzyme.

approach, using an STO-3G* basis set (Gaussian 94, Pittsburgh, PA), yielded a charge approximation with the simple peptide sequence Asp-Ser-Ala and the organophosphate linked to the serine. The amine on the Asp and carboxyl on the Ala were capped as neutral residues.

Molecular Dynamics and Energy Minimization of the Conjugated Phosphonates and the Reacting Oxime. Simulated anealing of the organophosphate conjugates was conducted in vacuo; side chains of AChE residues let free to assume energy minima are at positions 72, 74, 86, 121, 122, 124, 203, 204, 286, 295, 297, 337, and 347. Other side chains and the α-carbon backbone were fixed (*27*). Six starting positions for the OP with rotation increments of 60° around the $C_\beta-O_\gamma$ bond of Ser203 were used. The complex was originally minimized using 100 steps of conjugate gradients followed by 30 subsequent molecular dynamic time periods of 50 fs, starting at 700 K. The structures were cooled using steps of 50 K from 700 to 300 K. The dielectric constant was set at 4.0.

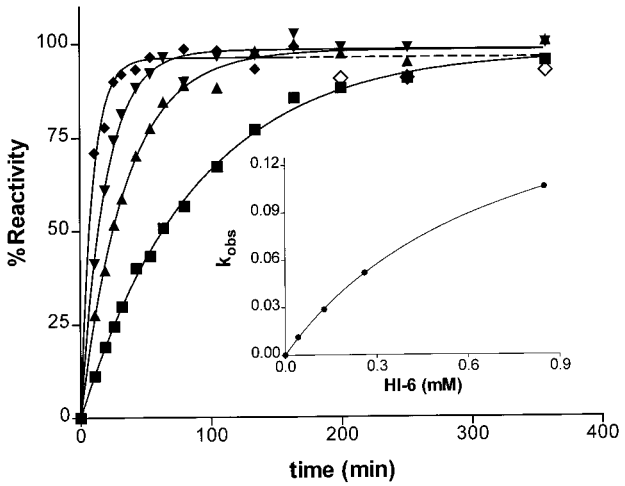

FIGURE 2: Reactivation of (S_p)-dimethylbutyl methylphosphonyl-AChE by HI-6. Purified mouse AChE expressed in transfected human embryonic kidney (HEK-293) cells was inhibited with (S_p)-dimethylbutyl methyl phosphonyl thiocholine to greater than 95% of the original activity. The enzyme was separated from reactants on a spin column. Oxime at the specified concentration was added to the diluted enzyme, and AChE activity was measured after designated times: (■) 0.0425, (▲) 0.128, (▼) 0.26, and (◆) 0.85 mM HI-6. In the inset, k_{obs} is plotted as a function of HI-6 concentration. Substitution of the data into eqs 1 and 2 yields the following values: $k_2 = 0.15$ min^{-1}, $K_{ox} = 0.83$ mM, and $k_r = 181$ M^{-1} min^{-1}.

RESULTS

Reactivation Kinetics. For the achiral inhibitor conjugate, dimethoxyphosphoryl-AChE, and the six enantiomeric conjugates, (R_p)- and (S_p)-cycloheptyl, (R_p)- and (S_p)-3,3-dimethylbutyl, and (R_p)- and (S_p)-isopropyl methyl phosphono-AChE (Figure 1),[2] a series of reactivation reactions were run over a wide concentration range to achieve saturation and determine K_{ox}, k_2, and k_r, the overall bimolecular rate constant (Figure 2).

Reactivation of the Achiral Phosphorate. The dimethoxyphosphoryl conjugate is formed by reaction of AChE with DDVP. The DDVP reaction yields the smallest, symmetrical organophosphate conjugate which serves as a reference for the bulkier chiral methylphosphonates. Data in Table 1 show similar rates of 2-PAM- and HI-6-elicited reactivation of the dimethylphosphoryl-conjugated enzyme. Modification of the two residues situated in the acyl pocket of AChE from the bulky aromatic groups to the aliphatic residues in BuChE at these positions reduces the bimolecular rate constant (k_r) slightly for the position 295 mutation and more dramatically for the position 297 mutation. Hence, oxime-elicited reactivation rates for the phosphoryl conjugate with small alkoxy moieties appear not to be enhanced by enlarging acyl pocket dimensions. Opening of the acyl pocket may simply provide more degrees of freedom of a conjugated phosphorate with relatively small substituent groups.

[2] Attack of the phosphorus by the serine with the thiocholine leaving group in the other apical position yields, in the absence of pseudorotation, a stereochemical inversion of the phosphorus upon forming the phosphoserine conjugate. Since thiocholine is the leaving group, the stereochemical nomenclature is reversed due to the higher order of the oxygen for the (R_p)- and (S_p)-cycloheptyl and isopropyl side chains. In the case of the 3,3-dimethylbutyl side chains, the order of the substituents does not change and the stereochemistry is not reversed. To avoid ambiguity, we designate all covalent conjugates via the configuration of the reacting alkylmethylthiocholine (*10*).

Table 1: Rate Constants for the Reactivation of Mouse Acetylcholinesterase Inhibited with DDVP[a]

enzyme	k_2 (min^{-1})	K_{ox} (mM)	k_r (M^{-1} min^{-1})	% reactivation
		2-PAM		
AChE	0.06	0.28	227	90−100
F295L	0.004	0.04	100	90−110
F297I	0.02	0.39	51	90−110
		HI-6		
AChE	0.02	0.19	113	90−100
F295L	0.005	0.09	56	90−110
F297I	0.01	0.36	28	90−110

[a] The kinetic constants represent the average or mean of two or more experiments. Individual determinations were typically within 10% of the average or mean value given in this and subsequent tables.

Table 2: Rate Constants for the Reactivation of Mouse Acetylcholinesterase Inhibited with S_p Enantiomeric Organophosphonates[a]

reactivator	enantiomer	enzyme	k_2 (min^{-1})	K_{ox} (mM)	k_r (min^{-1} M^{-1})	% reactivation
		Cycloheptyl Methylphosphonyl Thiocholine				
HI-6	S_p	AChE	0.36	2.0	186	96
HI-6	S_p	F295L	3.60	1.4	2520	94
HI-6	S_p	F297I	−	−	353	127
2-PAM	S_p	AChE	0.01	24	0.46	70
2-PAM	S_p	F295L	0.04	27	1.40	76
2-PAM	S_p	F297I	0.07	7.5	9.20	74
		3,3-Dimethylbutyl Methylphosphonyl Thiocholine				
HI-6	S_p	AChE	0.15	0.83	181	97
HI-6	S_p	F295L	1.70	1.30	1230	93
HI-6	S_p	F297I	0.14	0.44	318	120
2-PAM	S_p	AChE	0.042	179	0.24	104
2-PAM	S_p	F295L	0.038	35	1.10	103
2-PAM	S_p	F297I	0.190	6.4	30.0	102
		Isopropyl Methylphosphonyl Thiocholine				
HI-6	S_p	AChE	0.87	0.56	2160	91
HI-6	S_p	F295L	1.05	0.38	3320	105
HI-6	S_p	F297I	0.41	0.17	2400	102
2-PAM	S_p	AChE	0.130	0.83	155	99
2-PAM	S_p	F295L	0.043	0.37	116	107
2-PAM	S_p	F297I	0.740	0.95	779	92

[a] The kinetic constants represent the average or mean of two or more experiments. Dash denotes unresolved kinetic constants.

Reactivation of the Enantiomeric (S_p)-Phosphonates. Table 2 provides the kinetic parameters for reactivation of the AChE conjugates with the S_p enantiomers by 2-PAM and HI-6. K_{ox} and k_2 were determined from data similar to those depicted in Figure 2.

The maximal rate of reaction (k_2) is more rapid for HI-6, and coupled with its slightly smaller K_{ox}, this reactivator gives rise to a more rapid bimolecular rate constant, k_r, reflecting the comparative rates at low oxime concentrations. The rates for 2-PAM and HI-6 reactivation are greatest for the isopropyl methylphosphonyl conjugate which should present the least interference of the three (S_p)-phosphonates for oxime entry to the base of the gorge and attack on the phosphonyl oxygen. Moreover, this reactivation rate is also greater than that observed for the dimethoxy phosphorate (Table 1). Reactivation rates are 1−2 orders of magnitude slower for the (S_p)-3,3-dimethylbutyl and the (S_p)-cycloheptyl methyl phosphonate conjugates. The alkoxy moieties of the latter two compounds occupy larger volumes and should impart greater steric hindrance to the attacking oxime in the active center gorge.

Table 3: Rate Constants for the Reactivation of Mouse Acetylcholinesterase Inhibited with R_p Enantiomeric Organophosphonates[a]

reactivator	enantiomer	enzyme	k_2 (min^{-1})	K_{ox} (mM)	k_r (min^{-1} M^{-1})	% reactivation
		Cycloheptyl Methylphosphonyl Thiocholine				
HI-6	R_p	AChE	−	−	−	<25
HI-6	R_p	F295L	−	−	−	<25
HI-6	R_p	F297I	−	−	−	<25
2-PAM	R_p	AChE	−	−	−	<25
2-PAM	R_p	F295L	−	−	−	<25
2-PAM	R_p	F297I	−	−	0.005	92
		3,3-Dimethylbutyl Methylphosphonyl Thiocholine				
HI-6	R_p	AChE	0.24	1.9	117	86
HI-6	R_p	F295L[b]	0.0007	0.93	0.75	50
HI-6	R_p	F297I	−	−	−	<25
2-PAM	R_p	AChE	0.0130	28.0	0.52	77
2-PAM	R_p	F295L	0.0007	1.0	0.70	68
2-PAM	R_p	F297I	0.0008	2.1	0.40	74
		Isopropyl Methylphosphonyl Thiocholine				
HI-6	R_p	AChE	0.019	0.84	22.0	82
HI-6	R_p	F295L	0.001	0.97	1.03	101
HI-6	R_p	F297I	0.001	0.97	1.03	83
2-PAM	R_p	AChE	0.0120	0.40	36.0	89
2-PAM	R_p	F295L	0.0009	0.03	39.0	87
2-PAM	R_p	F297I	0.0008	1.03	0.77	134

[a] The kinetic constants represent the average or mean of two or more experiments. If the extent of reactivation is less than 25% over a 72 h period, individual constants were not determined and are denoted by a dash. [b] The reaction profile of F295L shows biphasic behavior; the slow phase represented by the constants above has the greater amplitude.

Substitution for the phenylalanines at the 295 and 297 positions with two aliphatic groups (F295L and F297I) should reduce the steric constraints in the gorge and improve access of the oxime to the conjugated phosphonate. Reactivation rates are accelerated by either of the two mutations, with the greater acceleration achieved for the conjugated inhibitors with more bulky alkoxy moieties (Table 2). However, acceleration is also oxime specific, with HI-6 reactivation rates enhanced by substitution for Phe295 and 2-PAM reactivation enhanced by substitution for Phe297. This suggests that the two oximes present themselves to the conjugated (S_p)-phosphonate with distinct attack orientations.

The mutations enhancing HI-6 reactivation rates appear to affect the maximum rate of reactivation, k_2, rather than the apparent dissociation constant of the oxime-conjugated AChE complex, K_{ox}. 2-PAM has a larger dissociation constant than HI-6, and acyl pocket mutations that enhance reactivation do so by decreasing K_{ox} and increasing k_2 to influence the bimolecular rate.

Reactivation of the Enantiomeric (R_p)-Phosphonates. Table 3 presents parallel reactivation rates for the R_p enantiomers with 2PAM and HI-6. For the bulky (R_p)-cycloheptyl methylphosphono-AChE conjugate, appreciable reactivation is not evident; only in the case of the F297I mutation is slow reactivation detected. With the 3,3-dimethylbutyl conjugate, slow reactivation is evident with HI-6 and 2-PAM; however, mutation of the acyl pocket residues does not enhance reactivation rates or the extent of reactivation. HI-6 only elicits partial reactivation for the F295L mutation, and its rate appears to be biphasic. The R_p compounds are known to be less reactive than the S_p enantiomers in forming the phosphonate conjugates (*15*), and all, but one, of the conjugates studied here reactivate more slowly. The isopropyl

Table 4: Rate Constants for the Aging of Mouse Acetylcholinesterase Inhibited with Respective Organophosphonates

enantiomer	enzyme	k_{aging} (min^{-1})	$t_{1/2}$ (h)
Cycloheptyl Methylphosphonyl Thiocholine			
S_p	AChE	0.00042	24
S_p	F295L	0.001	12
S_p	F297I	0.0037	31
R_p	AChE	NA[a]	NA
3,3-Dimethylbutyl Methylphosphonyl Thiocholine			
S_p	AChE	NA	NA
S_p	F295L	NA	NA
S_p	F297I	NA	NA
R_p	AChE	NA	NA
Isopropyl Methylphosphonyl Thiocholine			
S_p	AChE	0.0002	49
S_p	F295L	NA	NA
S_p	F297I	NA	NA
R_p	AChE	0.00045	27

[a] NA, no aging detected over the course of 72 h.

methylphosphonyl conjugates show the least alteration of the oxime dissociation constant (K_{ox}) or maximal (k_2) rates upon mutation of acyl pocket residues.

Aging and Spontaneous Reactivation of the Conjugates. Both 2-PAM and HI-6 have their oxime moieties ortho to the cationic pyridinium nitrogen, and their attacking orientations should have distinctive steric constraints (cf. Figure 1). Hence, the inability of 2-PAM and HI-6 to cause reactivation of certain R_p enantiomers may not reflect the capacity of all oximes for reactivation. Accordingly, we have conducted additional studies with obidoxime, a symmetric bifunctional compound, that has its oxime para to the pyridinium ring. Here, we find conjugates of the R_p compounds can be reactivated to near completion, but at very slow maximal rates: $k_2 = 0.002$ min^{-1} for the cycloheptyl conjugate, $k_2 = 0.14$ min^{-1} for the 3,3-dimethylbutyl conjugate, and $k_2 = 0.02$ min^{-1} for isopropyl conjugate. Appreciable reactivation seen with obidoxime indicates that aging of the conjugated phosphonate with the loss of the alkoxy group does not account for the resistance of the R_p compounds to reactivation.

Each organophosphate conjugate formed with the wild-type and mutant enzymes was examined for spontaneous hydrolysis and aging (Table 4). Rate constants for spontaneous hydrolysis in each case are considerably less than 0.001 min^{-1}. Hence, these rates are comparable to the rate of the loss of enzyme activity at 25 °C. Nevertheless, these slow rates show that general base-catalyzed hydrolysis is not contributing to the overall reactivation rate profiles.

Aging (i.e., the loss of an alkoxy moiety rendering an anionic conjugate resistant to oxime reactivation) was examined by measuring the extent of reactivation using high oxime concentrations added at designated intervals after inactivation with the phosphonate and removal of excess reactant. Table 4 shows the rates of aging seen for those compounds showing measurable reactivation rates with 2-PAM and HI-6. Aging rates are also relatively slow compared to the rates of oxime reactivation.

Energy Minimization of the Conjugated Phosphonates and Docking of the Oximes. Using the charges determined from the ab initio calculations for the respective organophosphates linked to the serine O_γ of the capped tripeptide, Asp-Ser-Ala, a second minimization was performed where the $C_{\alpha Ser}-C_{\beta Ser}-O_\gamma-P$ torsional angle of the conjugated Ser203 was started in the six positions on the enzyme differing by 60° (Figure 3), and side chains from residues 72, 74, 86, 121, 122, 124, 203, 204, 286, 295, 297, 337, and 447 were allowed to move freely. All other residues were fixed. The results of simulated annealing show that, for the majority of minimized structures, the phosphonyl oxygen for the S_p enantiomers moves to the oxyanion hole and the cycloheptyl group orients toward the choline site and gorge entrance. For the R_p enantiomers, the bulky group is forced from the acyl pocket to the gorge entrance, diminishing the interactions of the phosphonyl oxygen with the oxyanion hole (Figure 4). Proper positioning for hydrogen bonding of the phosphonyl oxygen depends on it residing within 3 Å of the amide backbone hydrogens of Gly121, Gly122, and Ala204. In the case of the R_p enantiomers, the cycloheptyl or another alkoxyl group resides within the gorge entrance, occluding potential oxime access. These phosphono−enzyme conjugates provide a basic template for docking of the two oximes (Figure 5).

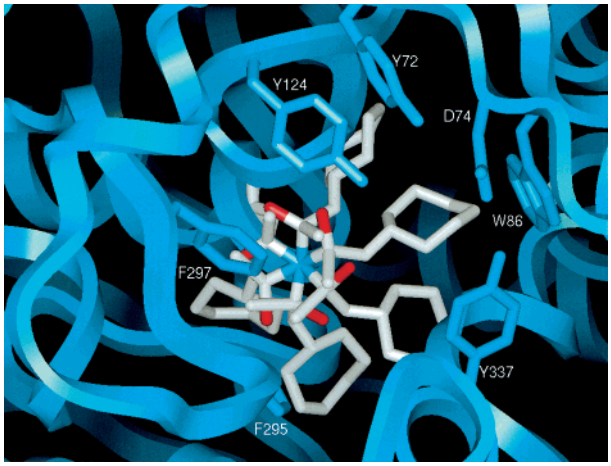

FIGURE 3: Starting positions of (S_p)-cycloheptyl methyl phosphonyl-AChE conjugates for energy minimization in the active center gorge. A starting conformation was built from conformations of congeneric organophosphates in the Cambridge Data Base. The leaving group is removed, and the phosphorus is attached to serine O_γ with 60° torsional rotations in the $C_{\alpha Ser}-C_{\beta Ser}-O_\gamma-P$ bond.

DISCUSSION

The availability of a three-dimensional structure of AChE (*12*−*14*) and its conjugates (*28*, *29*) enables one to examine reactivity in relation to the geometric confines of the active center. A comparison of reaction rates with enantiomeric phosphonates with known absolute stereochemistry is also of particular value, since in the absence of a dissymmetric enzyme active center, the two enantiomers should exhibit identical chemical behavior (*16*, *30*). Combining an understanding of the structure of AChE and its mutants with the enantiomeric selectivity of the phosphonates constitutes a powerful approach to delineating the orientation of the reactants involved in organophosphate inhibition and reactivation of AChE. Similar questions of chiral specificity have been approached with other enantiomeric organophosphates and hydrolases of the determined three-dimensional structure (*31*, *32*). Our analysis of the reactivation of the conjugates

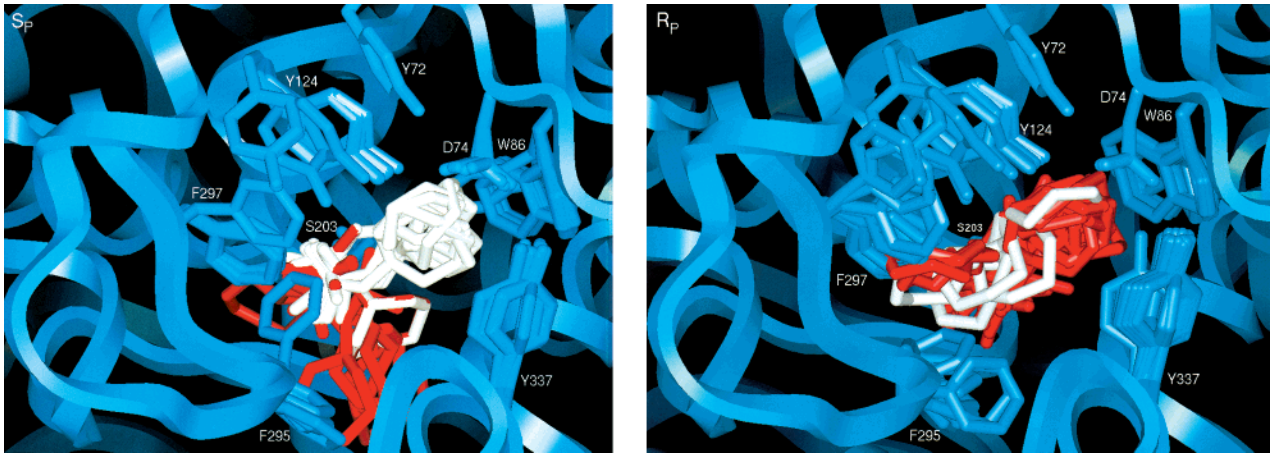

FIGURE 4: Energy-minimized conformation for (S_p)- and (R_p)-cycloheptyl methylphosphonyl-AChE. After energy minimization of the phosphonates as described in the text, they were conjugated to the serine with 60° torsional rotations around the $C_{\alpha Ser}-C_{\beta Ser}-O_{\gamma}-P$ bond (Figure 3). The figure shows the structures with the phosphonyl oxygen out of (red) and in (white) the oxyanion hole. The overlay shows the different conformation achieved after completing the cooling gradient: left, S_p conjugate; and right, R_p conjugate. In the case of the S_p stereochemistry, the phosphorus can be accessed from the gorge opening. The majority of S_p species maintain the phosphonyl oxygen directed in the oxyanion hole.

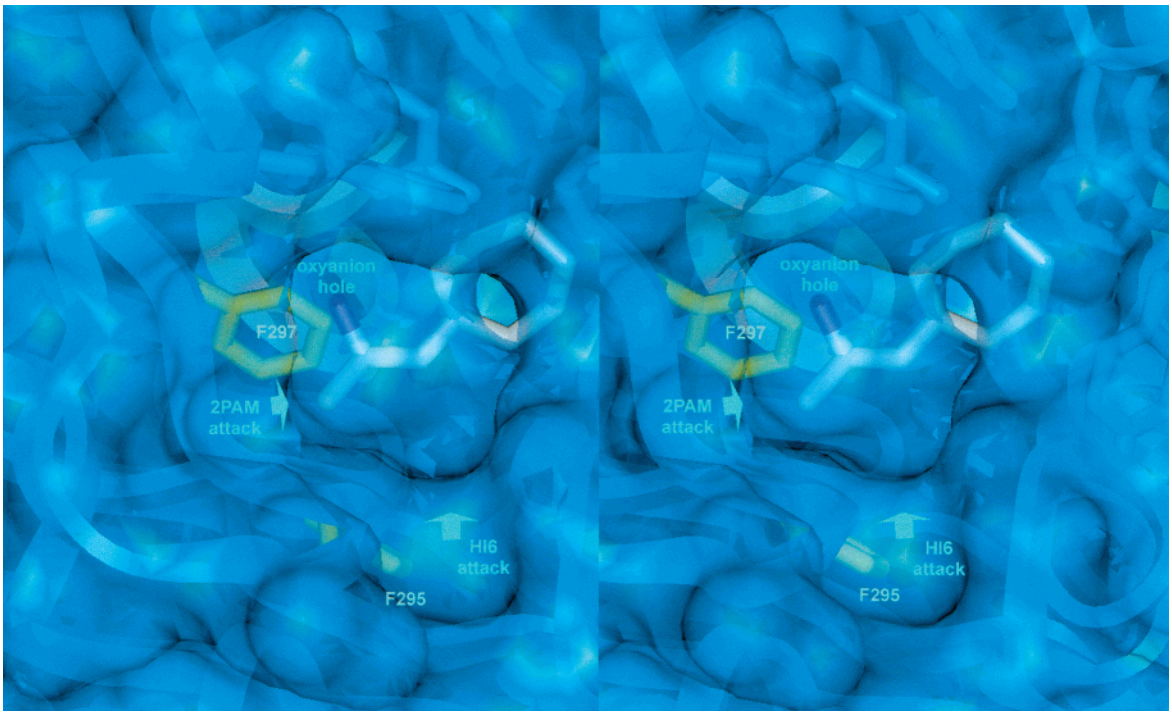

FIGURE 5: Stereoview with Conally surfaces of the proposed angle of access of 2-PAM and HI-6 to (S_p)-cycloheptyl methylphosphonate-conjugated AChE. The F295L mutation enhances the rate of reactivation by HI-6, whereas the F297L mutation enhances 2-PAM reactivation rates. Attack of the phosphorus can be optimized by substitution of phenylalanines in distinct positions. The orientation shows the gorge entry. The phosphonyl oxygen is shown in maroon; the cycloheptyl and methyl carbons are shown in yellow, and the α-carbon amide backbone of residues 120, 121, and 204 forming the oxyanion hole and the active center serine (203) are shown in white.

of chiral (R_p)- and (S_p)-phosphonates with the L-serine[3] in the active center reveals several distinctive features of the reactivation mechanism.

First, reactivation occurs more readily with the conjugated S_p enantiomers than with the R_p enantiomers. The (S_p)-phosphonates have been shown previously to be the more reactive enantiomer (*6*, *7*, *15*, *16*). If we assume an orientation where the leaving group is directed out of the gorge and where the phosphonyl oxygen is directed toward the oxyanion hole (*15*−*17*) and that this orientation facilitates the phosphonylation reaction, then the S_p enantiomers will have the small phosphonyl methyl moiety directed to the acyl pocket and the more bulky alkoxyl group directed to the choline subsite (Figure 4). The phosphonyl oxygen in the oxyanion hole is stabilized by hydrogen bond donors of amide bond hydrogens at positions 120, 121, and 204. With the R_p isomer, the same constraints on leaving group orientation and on phosphonyl oxygen binding in the oxyanion hole will force the alkoxyl group toward the space-confining acyl pocket. Steric limitations in the acyl pocket should relax the positional constraints of the phosphonyl

[3] The two asymmetric centers, located on the phosphonate and on L-serine 203, define the conjugates as diastereomers.

oxygen in the oxyanion hole and the leaving group exiting the gorge or distort the dimensions of the acyl pocket (*29*) (cf. Figure 4). Since oxime reactivation also prefers the S_p enantiomer, we might assume that orientation of the phosphonyl oxygen in the oxyanion hole facilitates the bond breaking associated with reactivation. Alternatively, distortion of the amino acid side chains necessary for accommodating the R_p enantiomer in the active center may yield a less reactive conjugate. In either case, the S_p enantiomer has its attached moieties with differing steric bulk better positioned for acylation and nucleophile-elicited deacylation of the serine. Maintaining the phosphonyl oxygen in the oxyanion hole is a critical consideration for both reaction mechanisms. However, for the R_p conjugates, this requirement forces the bulky alkoxy group into the gorge at a point of narrowing, further precluding access to the oxime (Figure 4).

The second feature stems from the relative resistance to reactivation for the methyl phosphonates substituted with larger alkoxy groups. The elegant studies of Wilson and colleagues showed that the efficiency of the oxime reaction is enhanced by site directing the oxime to the organophosphate through the use of cationic compounds resembling substrates or inhibitors (*1*, *2*). This finding takes on considerable practical significance since these oximes are the most efficacious agents in the treatment of organophosphate toxicity through reactivation of inhibited AChE (*3*, *35*). Oximes, being relatively strong nucleophiles, attack the electrophilic phosphorus, breaking the phosphoserine bond and forming an unstable phosphonyl oxime (*25*). Within the confines of AChE's narrow gorge, bulky organophosphates would be expected to lodge against the gorge wall, thereby limiting access of the oxime to the serine-conjugated phosphorus. The enhanced rate of reactivation of the S_p conjugates seen upon substitution for the aromatic groups in the acyl pocket with smaller and more flexible aliphatic groups presumably arises from increased oxime accessibility. The influence of the acyl pocket mutations also appears to be most dramatic for the larger cycloheptyl and dimethylbutyl moieties with little effect seen for the smaller isopropyl (Table 2) or methyl moieties (Table 1). Hence, steric limitations and impaction of the conjugate in the gorge are dominant factors in reducing oxime reactivation rates.

The combined requirement of the phosphonyl oxygen−oxyanion hole orientation and oxime accessibility to the phosphorus in the gorge provides an unusual constraint for reactivation of the conjugates of the R_p enantiomers. The orientation of the phosphonyl oxygen with respect to the oxyanion hole forces the alkoxy group to the space-confining acyl pocket or to the gorge exit. The former orientation may be precluded for the larger alkoxy moieties, while the latter limits access of the oxime through the gorge to the phosphorus.

The third feature is based on 2-PAM and HI-6 reactivity toward (S_p)-phosphonates being sensitive to the removal of spatial constraints at distinct positions in the acyl pocket. This suggests that the orientation of the two bound oximes and their angles of attack of the phosphorus differ. The likely attack directions for the two oximes under conditions where the acyl pocket is partially opened are shown in Figure 5. Since mutation of Phe297 to a smaller residue enhances 2-PAM reactivation and the Phe295 mutation affects HI-6 reactivation of the (S_p)-phosphonates, the accessibility to the phosphonate from two discrete directions preferentially facilitates oxime reactivity. Both reactivators have the attacking oxime situated ortho to the pyridinium nitrogen, but the HI-6 structure contains a second pyridinium moiety separated by a flexible 4.5 Å chain (Figure 1). This additional moiety with its cationic group can be expected to enhance affinity; however, it may also constrain the possible orientations of the attacking oxime.

Fourth, it is instructive to compare the rates of phosphonate inactivation and reactivation. Even after optimization of the reaction with a more open gorge, rates of bimolecular reactivation by oxime (Tables 1 and 2) appear to be relatively slow ($k_r = 10^2-10^3$ M^{-1} min^{-1}) compared to the rate of formation of the phosphonate conjugate with the serine ($k_r \sim 10^8$ M^{-1} min^{-1}). Analysis of the phosphonylation reaction by the phosphonate suggests a transition state orientation where the leaving group is directed out of the gorge and the hydrogen bond donors in the oxyanion hole delocalize the negative charge of the transition state (*15*, *16*). This creates near-optimal apical positioning of the attacking serine and leaving group in a pentavalent transition state. By virtue of the geometric constraints of the gorge, the efficiency of the oxime reactivation reaction appears to be limited by the attacking and leaving group not being in appropriate apical positions for forming an optimal transition state as is the case for phosphonylation by the phosphonate. Hence, even with facilitation of access of the oxime to the phosphonate, reactivation reactions may have intrinsic limits to their overall efficiency.

Our studies have examined only two oximes in detail, but the distinctions in kinetic constants for the series of organophosphates suggest that the rank order of potencies of the oximes in reactivation depends on the structure of the conjugated phosphonate. Others have observed in both in vivo and in vitro studies that oxime efficacies vary with the organophosphate inhibitor (*35*). Thus, antidote selection might be optimized by considering structure of the inhibitor. Overall, organophosphates with larger substituents may be the least amenable to oxime reactivation. The gorge dimensions create a substantial impediment to oxime access. In circumstances where combinations of oximes and AChE are considered to have catalytic potential in antidote therapy, enhanced reactivation rates and turnover of the conjugated phosphonate can be achieved with mutant enzymes that make the active center gorge more accessible to the attacking oxime.

REFERENCES

1. Wilson, I. B. (1959) *Fed. Proc. 18*, 752−758.
2. Wilson, I. B., and Ginsburg, S. (1975) *Biochim. Biophys. Acta 18*, 168−170.
3. Froede, H. C., and Wilson, I. B. (1971) in *The Enzymes* (Boyer, P. D., Ed.) Vol. 5, pp 87−114, Academic Press, New York and London.
4. De Jong, L. P. A., and Wolring, G. Z. (1984) *Biochem. Pharmacol. 33*, 1119−1124.
5. Benschop, H. P., Konings, C. A. G., Van Generen, J., and De Jong, L. P. A. (1984) *Toxicol. Appl. Pharmacol. 72*, 61−74.
6. Berman, H. A., and Decker, M. M. (1986) *J. Biol. Chem. 261*, 10646−10652.
7. Berman, H. A., and Decker, M. M. (1989) *J. Biol. Chem. 264*, 3951−3956.

8. De Jong, L. P. A., Verhagen, M. A., Langenberg, J. P., Hagedorn, I., and Loffler, M. (1989) *Biochem. Pharmacol. 38*, 633−640.
9. Hanke, D. W., Beckett, M. S., Overton, M. A., Burdick, C. K., and Leiske, C. M. (1990) *J. Appl. Toxicol. 10*, 87−91.
10. Berman, H. A., and Leonard, K. (1989) *J. Biol. Chem. 264*, 3942−3950.
11. Berman, H. A. (1995) in *Enzymes of the Cholinesterase Family* (Quinn, D. M., Balasubramanian, A. S., Taylor, P., and Doctor, B. P., Eds.) pp 177−182, Plenum Press, New York.
12. Sussman, J. L., Harel, M., Frolow, F., Oefner, C., Goldman, A., Toker, L., and Silman, I. (1991) *Science 253*, 872−878.
13. Bourne, Y., Taylor, P., and Marchot, P. (1995) *Cell 83*, 503−512.
14. Cygler, M., Schrag, J. D., Sussman, J. L., Harel, M., Silman, I., Gentry, M. K., and Doctor, B. P. (1993) *Protein Sci. 2*, 366−382.
15. Hosea, N. A., Berman, H. A., and Taylor, P. (1995) *Biochemistry 34*, 11528−11536.
16. Hosea, N. A., Radić, Z., Tsigelny, I., Berman, H. A., Quinn, D. M., and Taylor, P. (1996) *Biochemistry 35*, 10995−11004.
17. Taylor, P., Hosea, N. A., Tsigelny, I., Radić, Z., and Berman, H. A. (1997) *Enantiomer 2*, 249−260.
18. Ordentlich, A., Barak, D., Kronman, C., Benschop, H. P., De Jong, L. P., Ariel, N., Barak, R., Segall, Y., Velan, B., and Shafferman, A. (1999) *Biochemistry 38*, 3055−3066.
19. Taylor, P., Wong, L., Radić, Z., Tsigelny, I., Bruggeman, R., Hosea, N. A., and Berman, H. A. (1999) Esterases Reacting with Organophosphorus Compounds, *Chem.-Biol. Interact. 119*, 3−15.
20. Ashani, Y., Radić, Z., Tsigelny, I., Vellom, D. C., Pickering, N. A., Quinn, D. M., Doctor, B. P., and Taylor, P. (1995) *J. Biol. Chem. 270*, 6370−6380.
21. Grosfeld, H., Barak, D., Ordentlich, A., Velan, B., and Shafferman, A. (1996) *Mol. Pharmacol. 50*, 649−649.
22. Radić, Z., Pickering, N. A., Vellom, D. C., Camp, S., and Taylor, P. (1993) *Biochemistry 32*, 12074−12084.
23. Ellman, G. C., Courtney, K. D., Andres, V., Jr., and Featherstone, R. M. (1961) *Biochem. Pharmacol. 7*, 88−95.
24. Aldridge, W. N., and Reiner, E. (1972) in *Enzyme Inhibitors as Substrates* (Neuberger, A., and Tatum, E. L., Eds.) North-Holland Publishing Co., Amsterdam and London, and American Elsevier Publishing, New York.
25. Luo, C., Saxena, A., Smith, M., Garcia, G., Radić, Z., Taylor, P., and Doctor, B. P. (1999) *Biochemistry 38*, 9937−9947.
26. Cambridge Crystal Structure Data Base.
27. Brüggemann, R. J. M. (1999) Masters Thesis, University of Utrecht, Utrecht, The Netherlands.
28. Harel, M., Quinn, D. M., Nair, H. K., Silman, I., and Sussman, J. L. (1996) *J. Am. Chem. Soc. 118*, 2340−2346.
29. Millard, C. B., Kryger, G., Ordentlich, A., Greenblatt, H. M., Harel, M., Raves, M. L., Segall, Y., Barak, D., Shafferman, A., Silman, I., and Sussman, J. L. (1999) *Biochemestry 38*, 7032−7039.
30. Eason, L. M., and Stedman, E. (1933) *Biochem. J. 27*, 1257−1266.
31. Abend, A., Garrison, P. N., Barnes, L. D., and Frey, P. A. (1999) *Biochemistry 38*, 3668−3676.
32. Hong, S. B., and Raushel, F. M. (1999) *Biochemistry 38*, 1159−1165.
33. Cygler, M., Grochulski, P., Kazlankas, R. J., Schrag, J. D., Bouthillier, F., Rubin, B., Serreqi, A. N., and Gupta, A. K. (1994) *J. Am. Chem. Soc. 116*, 3180−3186.
34. Lang, D. A., Mannesse, M. L. M., DeHass, G. H., Verheu, H. M., and Dijkstra, B. W. (1998) *Eur. J. Biochem. 254*, 333−340.
35. Worek, F., Widmann, R., Knopff, O., and Szinicz, L. (1998) *Arch. Toxicol. 72*, 237−243.

BI992906R